Application of wavelet domain Markov random field model in THz image processing

Xing Liyun[1,2], Zhang Jin[1], Cui Hongliang[1]

(1. College of Instrumentation & Electrical Engineering, Jilin University, Chanchun 130022, China;
2. College of Electrical and Information Engineering, Beihua University, Jilin 132013, China)

Abstract: The main challenges for free-space terahertz (THz) imaging are known to be atmospheric loss, moisture absorption, low radiation power; and concequently, low signal-to-noise ratio (SNR). The need to have higher power radiation sources; faster data acquisition times remain major obstacles for high image quality. In this paper, the current state of research and applications was analyzed, as well as the future development of THz imaging technology was predicted. The basic principle of synthetic aperture radar (SAR) imaging and THz compressed sensing (CS) imaging was expounded. The THz image features of the two imaging methods were analyzed. The denoising effects of THz simulation images among the Wiener2, ddencmp, Donoho and the wavelet coefficients Amplitude Asymptotically Optimal (AAO) algorithm were also compared, qualitatively. A Markov random field(MRF) model for THz image denoising was presented, in order to capture the characteristics of scale space, with better scale wavelet coefficients in the wavelet domain. The image′s MRF model was established and the energy functions which were used for image denoising and the two states of each wavelet coefficient were introduced, in non-stationary regions: one state corresponded to the image features such as edge, while another state was related to the stationary region image. The Expectation Maximization (EM) algorithm was used to estimate the parameters of the mixture model, along with the Bayes Preliminary rule to determine the ideal image wavelet coefficients contraction factor. The denoising algorithm of the Hidden Markov Models in Wavelet Domain (HMMWD) was tested, with excellent simulation results that show the WDHMM to be more effective.

Key words: THz image processing; hidden Markov model; wavelet domain; denoising; Markov random field

CLC number: O799 **Document code:** A **Article ID:** 1007-2276(2014)07-2324-11

小波域马尔可夫随机场在THz 图像处理中的应用

邢砾云[1,2],张 瑾[1],崔洪亮[1]

(1. 吉林大学 仪器科学与电气工程学院, 吉林 长春 130022;
2. 北华大学 电气信息工程学院, 吉林 吉林 132013)

摘 要: 目前 THz 自由空间成像面临的挑战主要有大气损耗和水分吸收,辐射功率低,成像要获得高的信噪比,需要有更高功率的辐射源;数据获取时间长;图像质量仍需改善。分析了 THz 成像技术的最新发展趋势及国内外发展现状。阐述了利用 THz 辐射进行合成孔径成像、THz 压缩感知成像的基本原理,

收稿日期:2013-11-04; **修订日期**:2013-12-07

基金项目:重庆科委基础研究计划重大项目(cstc2013jcyjC00001)

作者简介:邢砾云(1981-),女,博士生,研究方向为 THz 成像及处理技术、SPR 传感及检测。Email:xingliyun116@foxmail.com

并对两种种成像方法形成的 THz 图像的特点进行了分析。应用 Wiener2,基于熵标准的 ddencmp 选定小波系数阈值降噪法、Donoho 提出的小波系数阈值降噪法以及基于小波系数幅值渐近最优降噪法等图像降噪算法对 THz 图像进行处理效果从均方根误差、信噪比、相关系数等方面进行了定性、定量的比较。提出将小波域马尔可夫随机场应用于 THz 图像降噪中。主要完成了以下几个方面:对每个小波系数引入两个状态,一个状态对应图像的非平稳区域,如边缘;另一个状态对应图像平稳区。每个状态下的小波系数用高斯分布函数来描述,虽然每个状态下的小波系数服从高斯分布,但每个小波系数的两个状态混合模型服从非高斯分布。然后利用 EM(Expectation Maximization)算法估计混合模型中的参数,采用贝叶斯准则初步确定理想图像小波系数的收缩因子。最后将小波域隐马尔可夫模型的降噪算法进行对比试验,仿真结果表明小波域隐马尔可夫模型的降噪算法更具有效性和优异性。

关键词: THz 图像处理; 隐马尔可夫模型; 小波域; 降噪; 马尔可夫随机域

0 Introduction

Presently, the main challenges for THz imaging are atmospheric loss and moisture absorption, low radiation power of the sources, low signal-to-noise ratio (SNR) at the detectors, and long data acquisition times. As the THz wavelength is several orders of magnitude higher than those of visible and infrared light, spatial resolution of the image is limited. Improvement of the image resolution often comes at the expense of the SNR. Image acquisition rate and spatial resolution for THz imaging remain major problems to be solved for wider applications of this promising technology.

A significant deficiency of the pulsed THz wave imaging is that the data acquisition time is too long. As a result, continuous wave (CW) THz imaging began to attract widespread attention[1]. Along with the CW THz imaging technology research and development, which in many fields have pushed it closer to practical use, demands for higher quality of CW THz image are becoming apparent. Complex characteristics of the CW THz images also require new methods suitable for CW THz image processing to meet the needs required of its applications.

1 Current state and development trend of THz imaging and processing

1.1 Recent progress of research in THz wave imaging

In recent years, with the development of THz source and detection technology, faster, increasingly portable, and wider applications of THz imaging are approaching reality. In order to improve the image acquisition rate and spatial resolution, the CS approach and the SAR THz imaging were developed, with the potential in accelerating imaging speed and improving spatial resolution[2-3].

It has been recognized earlier that THz imaging has the merit to produce a relatively large number of pixels based a finite number of THz detectors. In addition, it also has video imaging capability, making it possible to realize real-time monitoring of hidden explosives or other dangerous substances[2]. A unique THz imaging system can be designed similarly to digital camera or digital video camera[3].

Recently, SAR technology has been adopted for THz radar imaging[4]. There has been research on the THz SAR in the spatial and frequency domain, and analysis of the performances of the image reconstruction and operation time in the spatial and frequency domain. 3D high resolution THz SAR images have reconstructed using simulation data[5-6].

It has also been pointed out that THz digital holography is an effective method to eliminate the influence of diffraction. The lensless imaging characteristics of THz holography can avoid the loss and the lens distortion, and the associated difficult adjustment in the process of imaging, promising enormous application potentials[7-8].

Compared with traditional methods of THz

imaging, CS has been able to g reatly improve the imaging speed. Nonetheless, it is still limited by its scanning speed. Attempts have been made to improve the CS THz imaging system, using spatial random template modulation mechanism, leading to increased imaging speed[8], with the attendant increase in system complexity. Imaging method of coherent optical computing based on THz CS has been reported[3], as having a preliminary study on THz CS imaging[9], THz CW imaging experiments with backward wave oscillator (BWO), and others.

1.2 Current status of THz image processing

Characteristics of CW THz image with low contrast and uncertainty about its noise characteristics have posed great challenges to the processing work of CW THz image. Recent studies of a variety of interference factors in the THz image have produced more intuitive and reliable image information.

Stick filter has been employed to filter the amplitude and phase of images of composite materials. With this method effective detection of materials in the case of the noise with uncertain characteristics can be obtained. Using decomposition and synthesis process, the original information can be well preserved[8].

The wavelet transforms were used to filter out the stripes of CW THz image, as have various other methods of image processing in CW THz images, along with studies of processing methods to eliminate the stripes by Fourier transform (FT) and a variety of CW THz image enhancement algorithms. The method of neural network has been proposed for CW THz image recognition. It has been demonstrated that automatic detection of defects inside materials by THz CW source, combined with BP neural network can be achieved[1]. Analysis of the noise characteristics of CW THz image, followed by experimental results shows that statistical properties of the CW THz image′s noise is similar to the Gauss distribution[10]. Using the Wiener filter and mean filter processing, better image quality showing clear and obvious features was achieved[1].

2 Basic principles of SAR and THz imaging

2.1 SAR THz

SAR imaging is a high resolution radar imaging technology, which uses the pulse compression technique to obtain high range resolution, and synthetic aperture principle for high azimuth resolution. The formation of the large area and high resolution radar image enhances radar′s information acquisition capability, especially the battlefield awareness ability. However, with THz radiation, the wavelength is much smaller than those of microwave and millimeter wave, making it more suitable for attaining maximum signal bandwidths and extremely narrow antenna beams, useful for high resolution imaging of the targets.

The theory underlying the SAR imaging technique combined with THz technology can be summarized as follows (Fig.1). The 2D scanning is perpendicular to the beam direction, to obtain the high resolution THz image. Depth information of images can be obtained, namely the depth resolution. The 3D image of the object scene can be reconstructed, so SAT imaging in Non-destructive Testing (NDT) and recognition has great potential for development.

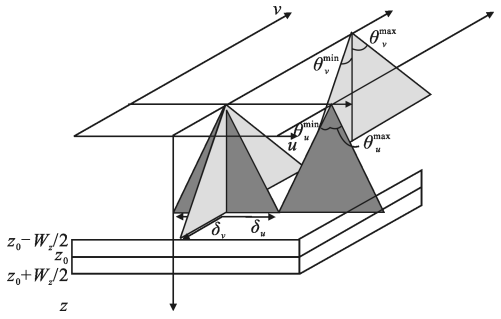

Fig.1 Geometry of SAR imaging[4]

2.2 CS THz imaging

CS takes a sparse high dimensional signal projects onto a low-dimensional space and through a certain linear or nonlinear decoding model to reconstructing the original signal with very high probability.

Through the sparse sampling of Fourier coefficient matrix, combined with the classical phase

compensation method, will take a number less than the traditional characteristics of image reconstruction. It has confirmed that of the CS theory in THz Imaging development potential.

Different from the traditional Nyquist theorem, in the framework of the CS theory, as long as the signal is compressible or sparse in a transform domain, the reconstruction of the original signal with the high probability by solving an optimization problem from small projections is possible. Schematic of THz imaging system based on CS theory is shown in Fig.2.

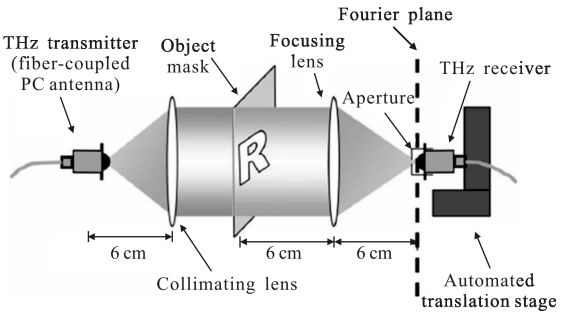

Fig.2 Schematic of THz imaging system based on CS[9]

3 THz image features

Point-by-point scanning is used in the process of CW THz imaging for the most part. The image acquisition process depends on the laser output, the atmospheric transmission, the optical system processing, the photoelectric conversion, and the computer processing. In accordance with the actual results, the analyses of the CW THz image characteristics are as follows[11]:

(1) The noise features of the image are fairly complicated. The THz imaging using the active scanning method is different from the optical passive imaging mode. Noises come from not only the process of transmission, detection and quantification, but also the light source output stability and mechanical scanning system stability. Such diverse sources of noises contribute to the complexity of the noise properties of CW THz image.

(2) THz imaging suffers from inherently low contrast: in practical applications, mostly involving imaging through obstacles, imaging beam attenuation and background light effect are prominent, leading to images with low contrast and/or ambiguous visual details.

(3) Current THz imaging technology is known to feature relatively low spatial resolutions. Considering wavelengths alone, according to the Rayleigh criterion, THz imaging should have relative higher spatial resolution, in contrast microwave and millimeter wave imaging. By the same reasoning, it is inferior to visible and infrared light. Imaging based on the point scanning approach makes the image resolution dependent upon the THz beam diameter. Due to the limit of the CW THz source, beam aperture cannot reach the lower value, so that the THz image resolution is poor.

(4) Stripes often appear in THz images. Previous analyses have shown that the stripes are the results of coherent, multiple, and other complex reflections of THz radiation, leading to spatial radiation modulation at the detector. As such, it can be considered as interference patterns.

According to fluctuation image of the pixels´ value as shown in Fig.3, we can know that the speckle noise is rarely. And the grayscale histogram of the background region is similar to the Gauss type.

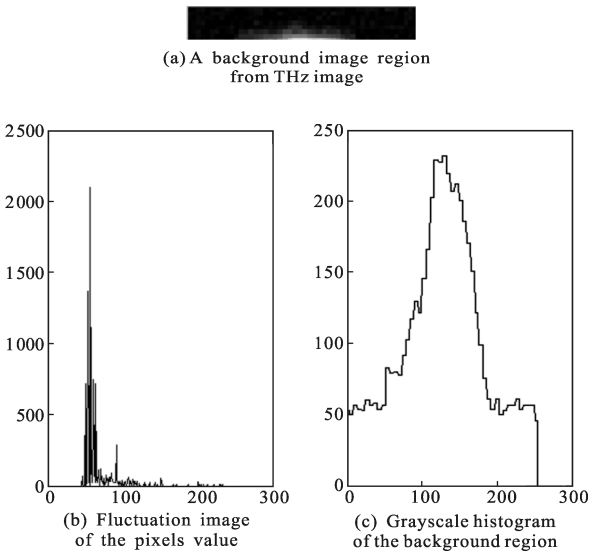

Fig.3 Noise analysis of THz image

From an analysis of previous experiments and

simulations, one can conclude that

(1) Speckle noise is rarely observed in THz imaging and its effect on the image can usually be ignored;

(2) The noise statistics of THz image obeys Gaussian distribution approximately, and can be modeled as such in practice.

4 Comparisons of the algorithms

The application of Wiener2, entropy standard ddencmp selected wavelet coefficient threshold denoising method , proposed by Donoho and based on the wavelet coefficients magnitude asymptotically optimal denoising method, from the root-mean-square error, signal-to-noise ratio, correlation coefficients of THz images for qualitative, quantitative comparison.

Analysis the de-noised effect, qualitatively. Wiener2 and ddencmp loss more details, the image is indistinct. The ddencmp is selected wavelet threshold with the standard entropy. It is the optimal threshold selection, when wavelet coefficients had equal probability. But the Lena wavelet coefficients size may not have equal probability, so the selected threshold is not the best, then loss more details. Denoising performance is restricted by the smoothing window size. At the same time as the Wiener filter coefficient was estimated using pixel values of noise pollution, so the filter coefficient deviates from the ideal of the Wiener filter coefficient, will cause the denoising effect of the image not ideal.

Using Donoho for denoising, details loss is relatively small. Because the Donoho threshold estimated the wavelet coefficients of ideal image, and then use the ideal wavelet coefficient to construct the Wiener filter. So the structure of the filter is close to the ideal filter. But because the Donoho threshold is global, it had a tendency to kill the wavelet coefficients, the wavelet coefficient estimated departure from ideal wavelet coefficients, leading to the denoising effect not ideal. Wavelet coefficients based on the AAO denoising method was firstly used to protect the edge of the image, and then was use in the asymptotic optimality of the threshold estimation wavelet coefficients of ideal image. The details of the denoising image lost were less than the other three methods. But there are still missing on the edges.

The effect among the different denosing algorithms were compared which were used in the THz simulation image Fig.4. And then three noisy image was shown in Fig.5–Fig.7. The THz simulation image with low noise SNR=25 dB and its denoising results is shown in the Fig.8. The THz simulation image with low noise $\sigma^2=0.002$ and its denoising results is shown in the Fig.9. The THz simulation image with low noise $\sigma^2=0.02$ and its denoising results is shown in the Fig.10.

Fig.4 Simulation image[11]

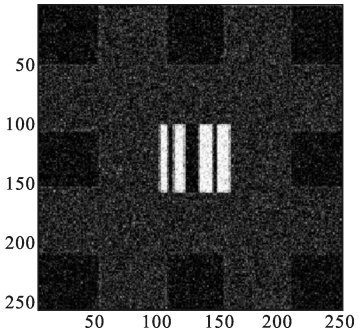

Fig.5 Noisy image1(SNR=25 dB)

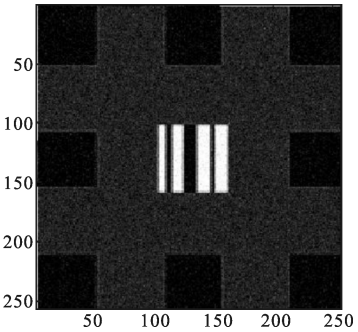

Fig.6 Noisy image2(σ^2=0.002)

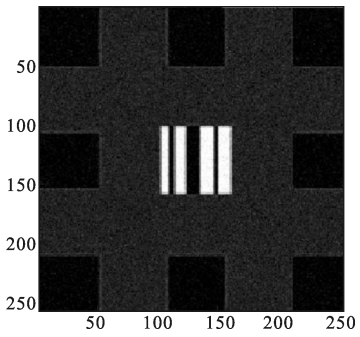

Fig.7 Noisy image3(σ^2=0.02)

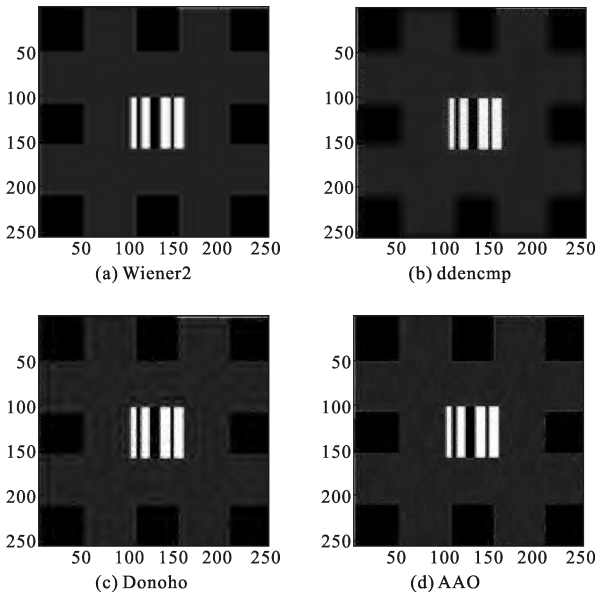

Fig.8 THz simulation image with low noise(SNR=25 dB) and its denoising results

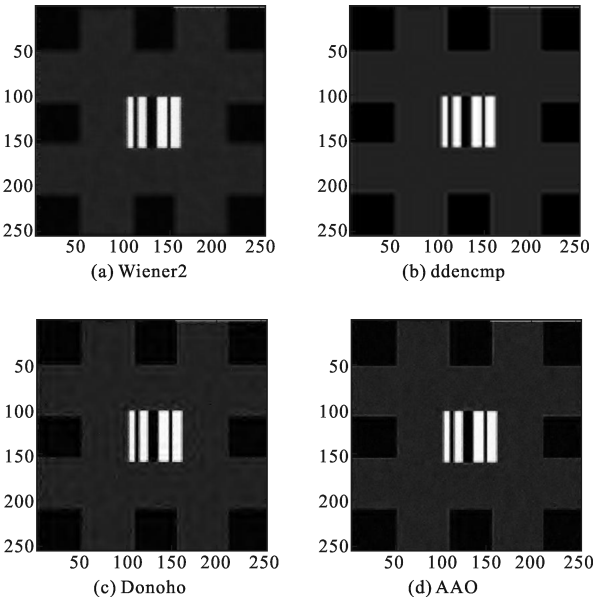

Fig.9 THz simulation image with low noise(σ^2=0.002) and its denoising results

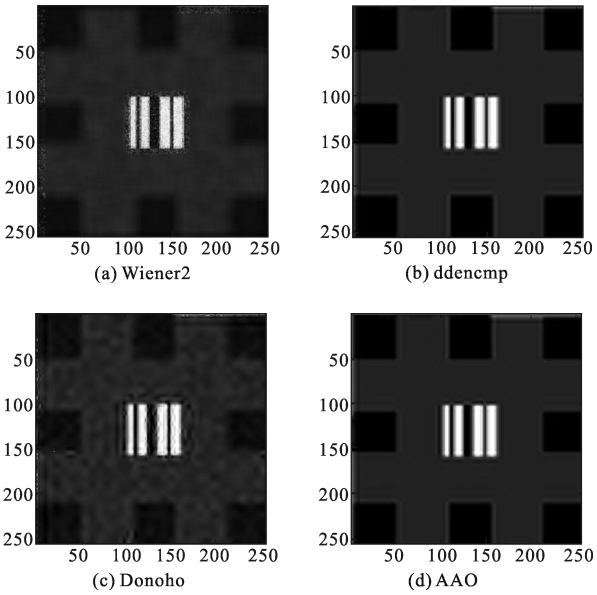

Fig.10 THz simulation image with low noise(σ^2=0.02) and its denoising results

A quantitative look at the de-noised effect, as shown in Tab.1, the MSE of the wavelet coefficient AAO denoising method is lowest; the de-noised images closest to the original image. When using ddencmp, the de-noised MSE is larger, it seems clear from the visual effect. Using Wiener2 for noise reduction, MSE is less than ddencmp denoising method, the visual effect is obvious. Looking from the de-noised SNR, wavelet coefficient AAO denoising method with the highest SNR, ddencmp is relatively low. The AAO COR method is the biggest, and closest to the original image, but ddencmp is least, as shown in the visual effect is obvious.

Tab.1 MSE, SNR and COR comparison of different methods

σ^2		Wiener2	ddencmp	Donoho	AAO
0.02	MSE	0.121 0	0.116 2	0.115 7	0.110 3
	SNR	24.300 1	20.453 9	25.216 1	26.151 8
	COR	0.948 21	0.932 54	0.950 12	0.956 68
0.002	MSE	0.029 8	0.030 0	0.020 9	0.019 8
	SNR	31.040 1	31.290 7	32.173 4	32.205 7
	COR	0.974 76	0.9523 1	0.985 55	0.987 76

Traditional low-pass filters to improve the image visual effects at the expense of high frequency information of image. The establishment of image

models accurately describe the image structure, in order to protect the crucial features of the image. In accordance with the characteristics of wavelet transform, there are scales space wavelet coefficient model, scale inside wavelet coefficient model and mixed model. The establishment of scale how accurate, scale wavelet coefficients in the model, is the bottleneck of improving the image noise reduction effect. Through the comparison of the algorithm above, according to the deficiencies of some model and the characteristics of wavelet transform, in order to capture the characteristics of the wavelet coefficients between scales and scale inside in the wavelet domain, a Markov random field is applied to THz image denoising.

5 HMMWD applied in the THz image processing

During the scanning amongst the adjacent points, the overlaps among the spot coverage areas will be caused by the restrictions of the facula effective aperture. Then the detection of information of a point contained the neighborhood information. And the two overlap points are not covered by the spot, their value will not affect each other. So it can be concluded that, in the CW THz scanning image, a pixel value is only related to its neighborhood, which is consistent with the definition of Markov random field. In other words, the THz image has the Markov property.

The reasons for the MRF model is introduced into the THz image processing:

(1) The THz image is consistent with the definition of Markov random field and has the Markov property. This laid the theoretical foundation for the application of MRF model in the processing of THz image.

(2) The MRF model can make the space between pixels tightly together, while the interaction between pixels is spread, so the image processing can be used in low order MRF to describe the relationship between pixels.

(3) MRF model can not only reflect the randomness o f the image, and can reflect the underlying image structure, which can effectively describe image properties.

(4) MRF is consistent with the physical model, and can connect with the image data fitting.

(5) When solved the uncertainty problem described in MRF, estimation theory of statistical decision theory, Bayesian is mainly used. First the prior knowledge of the image needs to be converted into the description of the prior distribution model, and then a posteriori estimation is used to obtain image optimization results. This process has the perfect mathematical derivation, and the results have clear physical meaning. The correctness of the solution can be verified by Monte Carlo method.

(6) Local characteristics of MRF model can be calculated by the massively parallel algorithms. In general applications of the THz system, the processing speed has little requirement, the delay in seconds is acceptable. The iterative nature of the algorithm could meet the requirements of the application of THz imaging system.

5.1 Finite Markov random field model build in wavelet domain[12]

Given the j−scale dyadic wavelet transform(DWT) of an $N*N$ image. The $3j+1$ various scales subbands is formed. The context structure of wavelet coefficients in the two-dimensional (2D) three-scale DWT, as show in Fig.9. The wavelet coefficient distribution is the reflections of the image regions.

Each subband coefficients can be described by the Gauss functions, and the entire subbands is considered to be the mixing of these Gauss functions. Namely, the probability distribution function can be characterized by the weighted sums of the each wavelet coefficient′s Gauss distribution function. This model is often called the finite normal-density mixture (FNM). The overall density function of w is given by

$$f(w_{ki}|r,s)=\sum_{v=1}^{V}\pi_v p(w_{ki}|\phi_v,s_{ki}) \tag{1}$$

Where w_{ki} denotes the wavelet coefficient of the pixel,

$\phi_v=(\mu_v,\sigma_v^2)$, $r=\{(\pi_v,\phi_v)\}$, $v=1,2,\cdots,V$, V is the number of the maximum possible status values.

$$p(w_{ki}|\phi_v)=(2\pi\sigma_v^2)^{-1/2}\exp\left[-\frac{(w_{ki}-\mu_v)^2}{2\sigma_v^2}\right] \quad (2)$$

Where μ_v, σ_v^2 and $p(w_{ki}|\phi_v,s_{ki})$ denotes the mean, variance and the probability distribution function when the wavelet coefficient at $s_{ki}=v$, $p(s_{ki}=v)=\pi_v$ are the weighted of the state components, $0<\pi_v<1$, $\sum_{v=1}^{V}\pi_v=1$.

Wavelet-domain hidden Markov models are multidimensional Gaussian mixture models in which the hidden states have a Markov dependency structure (as shown in Fig.11). Thus, the dependencies of wavelet coefficients can be captured through their hidden states. The parameters of the Wavelet-domain hidden Markov models(WHMM) can be expressed as:

Firstly, $A=\{a_{j,j+1}\}$ denotes the state transition probability distribution,

$$a_{jj+1}=p(s_{j,k,l}=v|s_{j+1,[k/2]_{MAX},[i/2]_{MAX}}=v') \quad (3)$$

Where a_{jj+1} denotes the state that transition from father to his children.

Secondly, $p(s_{ki}=v)=\pi_v$, is the probability distribution function of s_v.

Thirdly, calculate parameters μ_v, σ_v^2, at $s_{ki}=v$.

Lastly, calculate parameters $D=\{p_v(w_{ki})\}$ which denotes the wavelet coefficients of the observed values.

Then, the image′s Gaussian Hidden Markov Model (GHMM) in the Wavelet Domain is parameterized by:

$$\lambda^B=(A,\pi_v,D,\mu_v,\sigma_v^2) \quad (4)$$

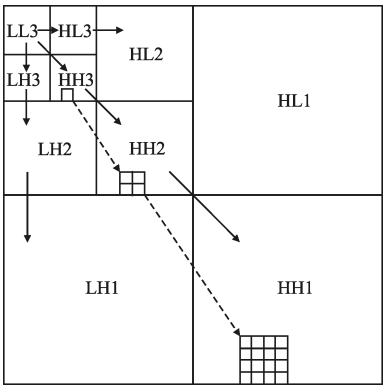

Fig.11 Two-dimensional (2-D) three-scale DWT

5.2 Bayes rule applied to estimating the desired image wavelet coefficients[12]

Under the condition of w_{ki} and using the GHMM, we estimate the desired image wavelet coefficients by:

$$\hat{y}=E[y_{ki}|w_{ki}]=\int y_{ki}P(y_{ki}|w_{ki})\mathrm{d}y_{ki}=\frac{\int y_{ki}P(w_{ki}|y_{ki})P(y_{ki})\mathrm{d}y_{ki}}{P(w_{ki})} \quad (5)$$

Where $P(y_{ki}|w_{ki})$ denotes the posterior probability of the desired image wavelet coefficients.

The prior probability of the desired image wavelet coefficients are defined by:

$$p(y_{ki})=\sum_{v=1}^{V}P(s_{ki}=v)P(y_{ki}|s_{ki}=v) \quad (6)$$

$$P(y_{ki}|s_{ki}=v)\sim n(0,\sigma_{xv}^2) \quad (7)$$

The prior probability of the observed image wavelet coefficients are defined by:

$$p(w_{ki})=\sum_{v=1}^{V}P(s_{ki}=v)P(w_{ki}|s_{ki}=v) \quad (8)$$

$$P(w_{ki}|s_{ki}=v)\sim n(0,\sigma_{wv}^2) \quad (9)$$

Where σ_{xv}^2, σ_{wv}^2 are the variance of the desired and observed image, respectively.

Then using formula(5)~(9), we obtain an empirical estimate for $\hat{y}_{ki}$ as

$$\hat{y}_{ki}=\sum_{v=1}^{V}P(s_{ki}=v|w_{ki})\frac{\sigma_{yv}^2}{\sigma_{wv}^2}w_{ki} \quad (10)$$

$$W_{ki}=\sum_{v=1}^{V}P(s_{ki}=v|w_{ki})\frac{\sigma_{yv}^2}{\sigma_{wv}^2} \quad (11)$$

Where $P(s_{ki}=v|w_{ki})\frac{\sigma_{yv}^2}{\sigma_{wv}^2}$ is called contraction factor.

The EM algorithm is used to estimate the contraction factor and the parameters of the model, according to the characteristics of the Markov model.

5.3 EM algorithms for training[12]

Step 1. Initialization:

Set the initial model parameters $\lambda^{B(t)}$, t is the number of iterations.

Step 2. E step:

Compute the mean of the complete data conditional probability by

$$Q(\lambda^{B},\lambda^{B(t)})=E_s[\ln f(w_{ij}^{B(c)},s|\lambda^{B})|w_{ij}^{B(c)},\lambda^{B(t)}]=$$

$$\sum_s f(s|w_{ij}^{B(c)},\lambda^{B(t)})\ln f(w_{ij}^{B(c)},s|\lambda^{B(t)})=$$

$$\sum_s f(s|w_{ij}^{B(c)},\lambda^{B(t)})\cdot[\ln f(w_{ij}^{B(c)}|s,\lambda^{B(t)})+\ln f(s|\lambda^{B(t)})] \quad (12)$$

Step 3. *M* step:

Update the model parameters.

$$\lambda^{B(t+1)}=\arg\max Q(\lambda^{B},\lambda^{B(t)}) \quad (13)$$

According to *E* step and *M* step, compute the posterior probability and model parameters by

$$f(s_k|w_{ij},\lambda^{(t)})=\frac{\pi_k^{(t)}f(w_{ij}|\lambda^{(t)})}{\sum_{k=0}^{1}\pi_k^{(t)}f(w_{ij}|\lambda^{(t)})} \quad (14)$$

$$\pi_k^{(t+1)}=\frac{1}{M/2^c\cdot N/2^c}\sum_{i=1}^{M/2^c}\sum_{j=1}^{N/2^c}f(s_k|w_{ij},\lambda^{(t)}) \quad (15)$$

$$\sigma_k^{2(t+1)}=\frac{1}{M/2^c\cdot N/2^c\pi_k^{(t+1)}}\sum_{i=1}^{M/2^c}\sum_{j=1}^{N/2^c}f(s_k|w_{ij},\lambda^{(t)})\cdot w_{ij}^2 \quad (16)$$

Step 4. Iterate:

Set $t=t+1$. If it converges, then stop. Otherwise, go to Step 3.

5.4 Wavelet coefficients partition[12]

The image is mainly composed of smooth region and non-stationary areas and the wavelet coefficient distribution is the reflections of the image structure. For the partition of the labels by the partition function as follows:

$$v(w)=\ln\frac{f(s=1)\dfrac{1}{\sqrt{2\pi}\sigma_{w1}}\exp\left(-\dfrac{w^2}{2\sigma_{y1}^2}\right)}{f(s=0)\dfrac{1}{\sqrt{2\pi}\sigma_{w0}}\exp\left(-\dfrac{w^2}{2\sigma_{y0}^2}\right)} \quad (17)$$

If $v(w)>1$, then $s=1$; otherwise, $s=0$.

Where the partition threshold is defined by:

$$T=\sqrt{\frac{\sigma_{w0}^2\cdot\sigma_{w1}^2}{\sigma_{w0}^2-\sigma_{w1}^2}\ln\frac{\pi_1\sigma_{w0}}{\pi_0\sigma_{w1}}} \quad (18)$$

Given the *T*, the label of the wavelet coefficient is initialized by

$$v_r=\begin{cases}1, & |w_{ij}|>T\\ 0, & \text{otherwise}\end{cases} \quad (19)$$

Consider the neighborhood wavelet coefficients and the features that the noise which easily formed the isolated point to remove the influence of noise on the label.

5.5 Contraction factor determination(Bayes rule) [12]

The Markov model is a powerful tool to describe the local interaction of the label field.

5.5.1 The ideal image labels determination

According to the local characteristics of Markov calculate(Bayes rule)

$$f(v_r|v_{\eta(r)})=\frac{1}{Z_2}\exp[-\alpha\sum_{\tau\in\eta(r)}\delta(v_r,v_\tau)] \quad (20)$$

Where Z_2 is normalization constant.

The local posteriori energy function:

$$u(v_r|v_{\eta(r)},w)\propto\left\{\left[-\frac{1}{2}\ln\sigma_{ws}^2-\frac{w_r^2}{2\sigma_{ws}^2}\right]+\alpha\sum_{\tau\in\eta(r)}\delta(v_r,v_\tau)\right\} \quad (21)$$

The ICM local optimization algorithm and the posteriori energy minimization function to get the labels of the wavelet coefficients.

$$\hat{v}_r^{t+1}=\arg\min u(v_r|v_{\eta(r)},w) \quad (22)$$

5.5.2 The ideal image wavelet coefficients determination

To characterize the initial value of the contraction factor in formula (11), it is necessary to have the wavelet coefficients in the ideal image. Resolving the weighted mean among the initial values of the contraction factors with the same label and then results were normalized to calculate the final contraction factor as follows:

$$\hat{\theta}_r=\frac{\sum_t\theta_t\delta(v_r,v_t)}{\sum_t\delta(v_r,v_t)} \quad (23)$$

Where $t=\{r,\eta(r)\}$, this results in the following equation are solved for $\hat{y}_r$.

$$\hat{y}_r=\hat{\theta}_r w_r \quad (24)$$

5.5.3 Denoising steps by the Markov contraction factor in wavelet domain

Step 1. The wavelet transform could be realized by selecting suitable wavelet basis function, and then the wavelet coefficients are obtained in various decomposition scales.

Step 2. Use formula (15)~(16) to confirm the parameters of $\lambda^{B}=(A,\pi_v,D,\mu_v\ \sigma_v^2)$, and then the value

of contraction will be computed the by fromula(11).

Step 3. Use formula (18) to confirm the partition threshold and get the initialized label by formula(19).

Step 4. Get the optimal label by formula(20).

Step 5. Use formula (21) to obtain the terminal contraction factor.

Step 6. Put the formula (21) results into formula (22), then we get the terminal denoising wavelet coefficient. Do the inverse wavelet transform to obtain the denoising image.

6 Simulation and analysis of the real example

In this paper, two states of each wavelet coefficient with non-stationary area are introduced, one state corresponding to the image such as edge, another state corresponding to stationary region image. The wavelet coefficient of each condition is described by a Gauss distribution function. Although the wavelet coefficient of each condition obeys Gauss distribution, the two mixed model state of each wavelet coefficient obeys non-Gaussian distributions. The EM algorithm is used to estimate the parameters of the mixture model, and the Bayes rule is employed to pre-determine the ideal image wavelet coefficients contraction factor. HMMWD are tested, with the simulation results showing that noise reduction algorithm in WDHMM is more effective and leads to excellent results. Denoising results of real CW THz scanning image is shown in Fig.12 and Tab.2. And Fig.13 has shown the denoising results of real CW THz scanning image with SNR=18.029 and SNR=26.996.

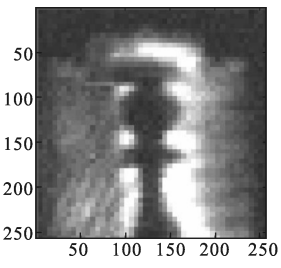

(a) CW THz scanning reflection image[12]

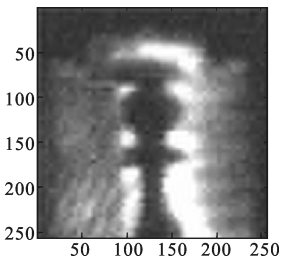

(b) Denoising result with WDHMM

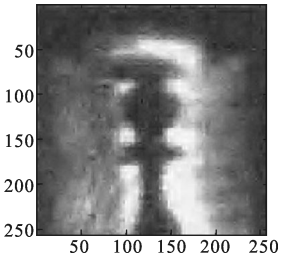

(c) Denoising result with AAO

Fig.12 Denoising results of real CW THz scanning image

Tab.2 Denoising results about MSE and SNR

Results	AAO	WDHMM
MSE	0.312 5	0.214 1
SNR	24.143 4	29.352 8

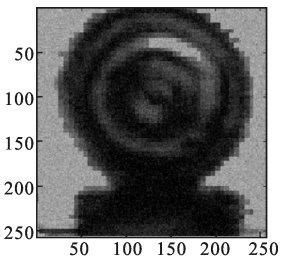

(a) CW THz scanning reflection image (SNR=18.029)

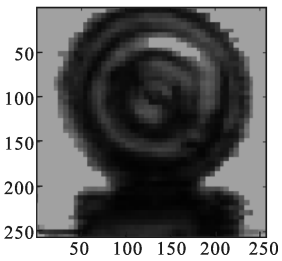

(b) Pretreatment image

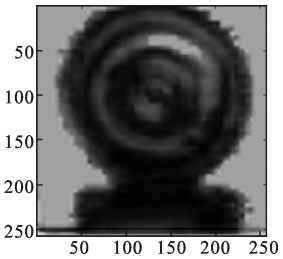

(c) Denoising result with WDHMM (SNR=26.996)

Fig.13 Denoising results of real CW THz scanning image

References:

[1] Li Qi, Yin Qiguo, Yao Rui, et al. Continuous-wave THz image denoising based on Markov random field and simulated annealing algorithm [C]//International Symposium on Photo electronic Detection and Imaging (SPIE), 2009, 04: 73850L.

[2] Heremans R, Vandewal M, Acheroy M. Synthetic aperture imaging extended towards novel THz sensors[C]//Proceedings of the IEEE Sensors 2008 Conference, 2008: 438-441.

[3] Li Xinlei, Li Biao. The technology of the real-time THz

detection and imaging advances [J]. ***Laser & Optoelectronics Progress***, 2012, 49: 090008. (in Chinese)

[4] Marijke Vandewal, Roel Heremans, Marc Acheroy. Synthetic aperture signal processing for high resolution 3D image reconstruction in the THz-domain [C]//Proceedings of the 17th European Signal Processing Conference (EUSIPCO), 2009, 13: 744-748.

[5] Ma Chaojie, Sun Xiaoquan, Li Xiaoxia. Simulation design of the radar guidance system based on the laser imaging [J]. ***Infrared and Laser Engineering***, 2005, 34(6): 655-659. (in Chinese)

[6] Cao Juncheng. Semiconductor THz source detector and its application[J]. ***Science Press***, 2012: 429-439.

[7] Li Yunda, Li Qi, Liu Zhengjun, et al. Simulation studies on computer-aided tomography terahertz image reconstruction algorithm[J]. ***Infrared and Laser Engineering***, 2013, 42(5): 1228-1235. (in Chinese)

[8] Ronan Mahon, Anthony Murphy, William Lanigan. Terahertz holographic image reconstruction and analysis [J]. ***Infrared and Millimeter Waves***, 2004, 27: 749-750. (in Chinese)

[9] Wai Lam Chan, Matthew L Moravcc, Richard G Baraniuk, et al. Terahertz imaging with compressed sensing and phase retrievalJ]. ***Opt Lett***, 2008, 33(9): 974-976.

[10] Shan Jixin. Primary investigation of terahertz scanning reflection imaging and real-time transmission imaging [D]. Harbin: Harbin Institute of Technology, 2009. (in Chinese)

[11] Yin X X, Ng B W-H, Ferguson B, et al. Wavelet based segment detection and feature extraction for 3D T-Ray CT pattern classification[C]//Digital Signal Processing Workshop, 12th-Signal Processing Education Workshop, 2006: 602-607.

[12] Li Xuchao. Application of Wavelet Domain Markov Random Field to Image Processing [M]. Beijing: Publishing House of Electronics Industry, 2011: 121-143. (in Chinese)